RESEARCH ARTICLE

Macromolecular Materials and Engineering
Open Access
www.mame-journal.de

Development and Characterization of Poly(butylene succinate-*co*-adipate)/Poly(3-hydroxybutyrate-*co*-3-hydroxyvalerate) with Cowpea Lignocellulosic Fibers as a Filler via Injection Molding and Extrusion Film-Casting

*Mondli Abednicko Masanabo, Amélie Tribot, Enni Luoma, Jussi Virkajärvi, Nusrat Sharmin, Morten Sivertsvik, Suprakas Sinha Ray, Janne Keränen, and M. Naushad Emmambux**

Biodegradable poly(butylene succinate-*co*-adipate)/Poly(3-hydroxybutyrate-*co*-3-hydoxyvalerate) (PBSA/PHBV) filled with lignocellulosic sidestream/fibers from cowpea, a neglected and underutilized African crop are produced by injection molding and extrusion film casting. Differential scanning calorimetry (DSC) and dynamic mechanical analysis (DMA) suggests that the fibers have more affinity and interfacial interaction with PBSA than PHBV. This is shown by a decrease in dampening of PBSA and an increase in dampening of PHBV with fiber addition. In addition, fiber addition results in more homogeneous crystal morphology of PBSA, while resulting in more heterogeneous crystal morphology of PHBV. The tensile strength of injection molded bio-composites increases with fiber addition due to good interfacial adhesion between the matrix and fibers revealed by scanning electron microscope. In contrast, the tensile strength of bio-composite films decreases with fiber addition due to the high-volume fraction of pores in bio-composite films that act as stress raisers. The stiffness of both injection molded, and bio-composite films increase with fiber addition, as revealed by an increase in Young's modulus and storage modulus, while the tensile strain decreases. In conclusion, low-value cowpea sidestream can be used as a filler to produce injection molded bio-composites and bio-composite films for potential application as rigid and flexible packaging.

1. Introduction

Plastics are ubiquitous in our everyday lives, with packaging accounting for a significant portion of our plastic consumption.[1] Unfortunately, of the total plastic waste generated, about 79% is mismanaged and accumulates in natural environments and landfills as pollutants. If current production and waste management practices remain unchanged, about 12 000 million metric ton of plastic will end up as waste in the environment by 2050.[2] Petroleum-based plastics account for about 97% of total plastics, the vast majority of which are not biodegradable and accumulate in the environment as waste.[3] These nonbiodegradable plastics are broken down by ultraviolet light and mechanical wear into microplastics that have adverse health effects on the environment, animals, and humans.[3,4] These environmental concerns pertaining to petroleum-based and nonbiodegradable plastics have prompted the need to develop environmentally friendly plastics that are biodegradable, recyclable, and from sustainable resources.[5]

M. A. Masanabo, M. N. Emmambux
Department of Consumer and Food Sciences
Faculty of Natural and Agricultural Sciences
University of Pretoria
Hatfield 0028, South Africa
E-mail: Naushad.emmambux@up.ac.za

A. Tribot, E. Luoma
VTT Technical Research Centre of Finland
Visiokatu 4, Tampere 33101, Finland

J. Virkajärvi, J. Keränen
VTT Technical Research Centre of Finland Ltd
Koivurannantie 1, Jyväskylä 40400, Finland

N. Sharmin
Department of Food Safety and Quality
Nofima AS, Osloveien 1, Ås 1430, Norway

M. Sivertsvik
Department of Processing Technology
Nofima AS, Richard Johnsens gate 4, Stavanger 4021, Norway

S. S. Ray
Centre for Nanostructures and Advanced Materials
DSI-CSIR Nanotechnology Innovation Centre
Council for Scientific and Industrial Research
Pretoria 0001, South Africa

DOI: 10.1002/mame.202400037

Biodegradable polymers made from sustainable and renewable resources are attractive alternatives to replace petroleum-based polymers. Among several commercially available bio-based, biodegradable polymers, poly(butylene succinate-*co*-adipate) (PBSA) is a promising candidate, as it has excellent melt processibility via various polymer processing techniques and has mechanical properties comparable to polyethylene.[6,7] However, its poor gas barrier properties compared to other biodegradable polymers, such as Poly(3-hydroxybutyrate-*co*-3-hydoxyvalerate) (PHBV) and polyglycolic acid (PGA) limits its application.[8,9] PHBV, on the other hand has good oxygen and water vapor barrier properties and generally improves the barrier properties of other biopolymers in a blend.[10] Furthermore, both PBSA and PHBV have excellent biodegradation properties in various environments.[11] Therefore, the blending of PBSA and PHBV is a feasible strategy to improve the properties of the individual polymers, to widen their application while maintaining biodegradation.

Both PBSA and PHBV can be completely bio-sourced, which makes them very attractive alternatives to petroleum-based polymers.[12] However, these bio-based polymers have a relatively high cost compared to most extensively used commercial biopolymers, such as or polylactide (PLA). An attractive solution to reduce the cost of PBSA and PHBV while improving their functionality and preserving biodegradability could be the addition of lignocellulosic fibers from agricultural waste to produce bio-composite plastics.[13]

Bio-composite plastics made from bio-based and biodegradable polymers have desirable properties, such as high stiffness, lightweight, and biodegradable.[14] The use of low-value agricultural waste from African crops as a filler in bio-composites is poorly documented in literature. In our previous work, agricultural waste from Faba bean (*Vicia faba L.*) milled to less than 2 mm was demonstrated as filler up to 30% loading in a PBSA/PHBV blend matrix.[15] In this work, we further expand on the use of agricultural waste from cowpea [*Vigna unguiculata* (L.) Walp], an indigenous African crop as a filler in PBSA/PHBV matrix to prepare injection molded bio-composite plastics and bio-composite films.

Cowpea is a legume that is largely grown in sub-Saharan Africa for food and animal feed, and it is one of the most economically important indigenous African legume crops.[16,17] Approximately 6.5 million metric tons of cowpea are grown worldwide on ≈14.5 million hectares of land.[17] Cowpea sidestream/residue is not traded as a commodity, and thus has no economic value as such. The value addition of agricultural residues has been shown to generate nonfood sources of economic development for farmers in rural areas and developing countries.[18]

To the best of our knowledge, there is no notable research that has utilized cowpea lignocellulosic fibers as a filler. Therefore, the objective of this work is to determine the effect of cowpea lignocellulosic fibers in a PBSA/PHBV blend matrix on the thermal, thermomechanical, morphological, mechanical, and barrier properties of injection molded bio-composites and bio-composite films, with the aim of producing biodegradable and bio-based injection molded bio-composites for rigid packaging and bio-composite films for flexible packaging.

2. Experimental Section

2.1. Materials

PBSA BioPBS FD92PM with a density of 1.24 g cm^{-3} and a melting point of 84 °C was procured from PTT MCC biochem Co., Ltd (Bangkok, Thailand). PHBV ENMAT Y100P with a density of 1.25 g cm^{-3} and a melting point of 170–176 °C, was procured from Helian Polymers (Belfeld, Netherlands). The cowpea lignocellulosic sidestream was obtained from a local farm (Farm Uitval, Vermass) in June 2021 in the North West province, South Africa, after the grains were harvested. The cowpea sidestream was washed with water, followed by drying in an oven at 40 °C for 24 h. This was followed by milling to less than 500 µm (**Figure 1**), vacuum packed, and stored in sealed containers until use. The cellulose and hemicellulose content of the cowpea sidestream was determined according to the method described by Carrier et al[19] and lignin was determined according to the LAP-003 method for acid insoluble lignin.[20] The cowpea lignocellulosic fibers contained 39% cellulose, 27% hemicellulose, and 13% lignin.

2.2. Processing of the Injection Molded Bio-Composites and Bio-Composite Films

The processing of injection molded bio-composites and bio-composite films is shown in Figure 1 and described in detail in the text. Before processing the cowpea sidestream was dried at 50 °C overnight to reduce moisture to less than 3%. Similarly, PBSA and PHBV were dried at 70 °C overnight before processing. PBSA and PHBV were mixed (85/15 ratio) in a bag and loaded into the first feeder, and the second feeder was loaded with dried cowpea lignocellulosic sidestream (Figure 1). About 4 kg of the bag mixed PBSA/PHBV blend and PBSA/PHBV containing 10%, 20%, and 30% w/w cowpea lignocellulosic sidestream/fibers were compounded into pellets using a twin-screw extruder (Berstorff ZE 25 × 33 D, Berstorff GmbH, Hanover, Germany) equipped with two feeders. The temperature profile in the twin-screw extruder was 80/165/175/175/175/175/175/175/175 °C (from feeder to die), the screw speed varied between 75 and 100 rpm with an output of 3 kg h^{-1}. The pellets were stored for further processing via film extrusion and injection molding.

Prior to further processing, the compounded pellets (Figure 1) were vacuum dried overnight at 60 °C. Dog-boned test specimens (Figure 1) were then prepared from the pellets according to the ISO 527-1 method (2019) using the injection mold (Battenfeld Smart Power 60-210, servo hydraulic machine, 60 ton clamping unit, 25 mm screw diameter). The mold temperature was 30 °C, while the screw temperature was 190/190/190 °C for the PBSA/PHBV blend and 5 °C higher for bio-composites containing fibers for sufficient melt flow properties and mold filling.

The dried pellets were also further processed into films using a 19 mm single-screw extruder (Barbender Plasti-corder, Germany) (Figure 1) equipped with a conical screw extruder with a 3:1 compression ratio. The screw temperature profile was 175/175/175/165/165/165 °C, screw speed 50 rpm and chill roll temperature of 40 °C. The melt temperature of 155–156 °C and

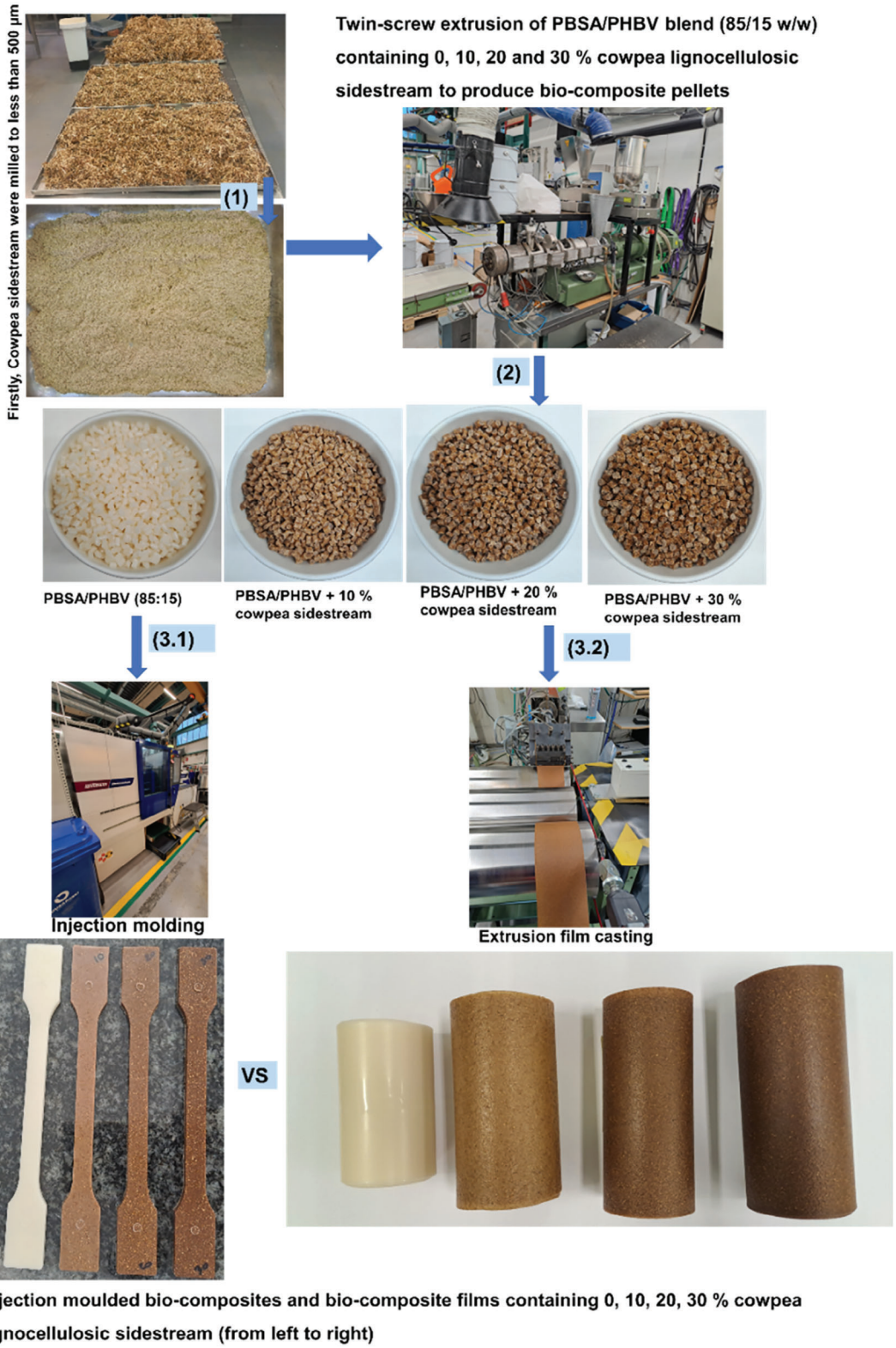

Figure 1. Processing steps to produce injection molded bio-composites and bio-composite films containing 0, 10%, 20%, and 30% cowpea lignocellulosic sidestream. Step 1 shows the milled cowpea sidestream, step 2 shows the compounding of polymers and fibers to produce bio-composite pellets; step 3.1 shows injection molding, and step 3.2 shows extrusion film casting.

torque of 10.4–10.6 N m were recorded during processing. The sheet die (Extron Mecanor Oy, Akaa, Finland) was 120 mm wide.

2.3. Characterization

2.3.1. Thermogravimetric Analysis (TGA)

The thermal stabilities of the injection molded bio-composite and bio-composite films were evaluated using TGA Q500 (TA Instruments, USA). About 8–10 mg of samples were weighed in platinum pans and heated from 30 to 700 °C at a heating rate of 10 °C min^{-1} under nitrogen gas.

2.3.2. Differential Scanning Calorimetry (DSC)

Differential scanning calorimetry DSC 2500 (TA Instruments, USA) was used to evaluate the thermal transitions of the injection molded and bio-composite films. About 5–6 mg samples were heated and cooled in 3 cycles. The samples were equilibrated at −50 °C and heated to 200 °C under nitrogen gas with a flow rate of 25 mL min^{-1}. The samples were held at 200 °C to erase thermal history. In the second cycle, the samples were cooled from 200 to −50 °C to analyze the crystallization behavior. The second heating was from −50 to 200 °C to evaluate melting behavior and crystallinity. The heating and cooling rate was constant at 10 °C min^{-1}. The degree of crystallinity (X_c) of PBSA and PHBV were evaluated using the equation

$$\mathrm{X}c = \frac{\Delta H\mathrm{m} - \Delta H\mathrm{cc}}{\Delta H^{\circ} \times \left(1 - \mathrm{W}f\right)} \times 100 \quad (1)$$

Where ΔH_m is the melting enthalpy, ΔH_{cc} is the cold crystallization temperature, ΔH° is the melting enthalpy of 100% crystalline polymer with PBSA (113.4 j g^{-1}) and PHBV (146 j g^{-1})[12] and W_f is the volume fraction of the corresponding polymer.

2.3.3. Dynamic Mechanical Analysis (DMA)

The thermomechanical properties of the injection molded, and bio-composite films were evaluated using DMA 800 (PerkinElmer, USA). The instrument was operated in a dual cantilever bending mode for injection molded bio-composites with dimensions (24.8 mm length × 9.8 mm width × 1.6 mm thickness) and operated in a tension mode for bio-composite films with dimensions (11 mm length × 8 mm width × ≈500 µm thickness). The samples were heated from −70 to 70 °C at a heating rate of 3 °C min^{-1} at a frequency of 1 Hz and 0.05 mm strain.

2.3.4. Scanning Electron Microscope (SEM)

The injection molded bio-composites and bio-composite films were freeze-fractured in liquid nitrogen. The freeze-fractured samples were sputter-coated with carbon. The morphology was evaluated using a field emission gun scanning electron microscope (FEG-SEM) Zeiss 540 Ultra (Zeiss, Germany) at an accelerating voltage of 2 kV.

2.3.5. X-Ray Tomography

The 3D X-ray tomography images of the injection molded, and bio-composite films were captured using RX Solutions Desktom 130 (RX Solutions, Chavanod, France). The instrument was operated with an acceleration voltage of 40 kV. The X-ray tube current, the imager frame rate, and the reconstructed image pixel size were 119 mA, 1 Hz, and 5.6 µm for dog-boned samples and 110 mA, 0.75 Hz, and 4 µm for film samples, respectively. Each 360° scan contained 1440 projection images and RX Solutions XAct software was used in the filtered back projection algorithm reconstruction. The volume fractions of the pores were calculated from the 3D image data using VTT in-house analysis software. More details of the image analysis are given in the Supporting Information.

2.3.6. Tensile Properties

The tensile properties of injection molded bio-composites (dog boned in Figure 1) were tested according to ISO 527-1 (2019) standard using an Instron 4505 Universal Tensile Tester (Instron Corp., Canton, MA) equipped with a 5 kN load cell and an Instron 2665 Series High-Resolution Digital Automatic Extensometer (Instron Corp., Canton, MA). A crosshead speed of 5 mm min^{-1} was used, and about 6 specimens were tested for each sample.

The tensile test specimen of the bio-composite films was prepared according to ASTM D882-18 (2018) in the form of strips (50 mm length and 20 mm width). The tensile properties of the bio-composite films were evaluated using an Instron 5964 Universal Tensile Tester (Instron Corp., Canton, MA) equipped with a 2 kN load cell. A crosshead speed of 100 mm min^{-1} was used, and about 6 specimens were tested for each sample.

2.3.7. Water Vapor Permeability (WVP)

About 5 cm^2 bio-composite film samples were cut and evaluated for water vapor transmission rate using Dualperm 7002 (Industrial Physics, Johnsburg, IL), measured 23 °C, 85% RH. WVP was calculated from the water vapor transmission rate. Four parallels were measured per sample.

2.3.8. Oxygen Permeability (OP)

About 5 cm^2 bio-composite film samples were cut and evaluated for oxygen transmission rate using a Dualperm 8001 instrument (Industrial Physics, Johnsburg, IL) measured at 23°C, 50% RH. OP was calculated from the oxygen transmission rate. Four parallels were measured per sample.

2.4. Statistical Analysis

The version 20 IBM SPSS version 20 statistical software (Armonk, NY: IBM Corp.) was used for statistical analysis of the data. Multifactor analysis of variance was used to evaluate the

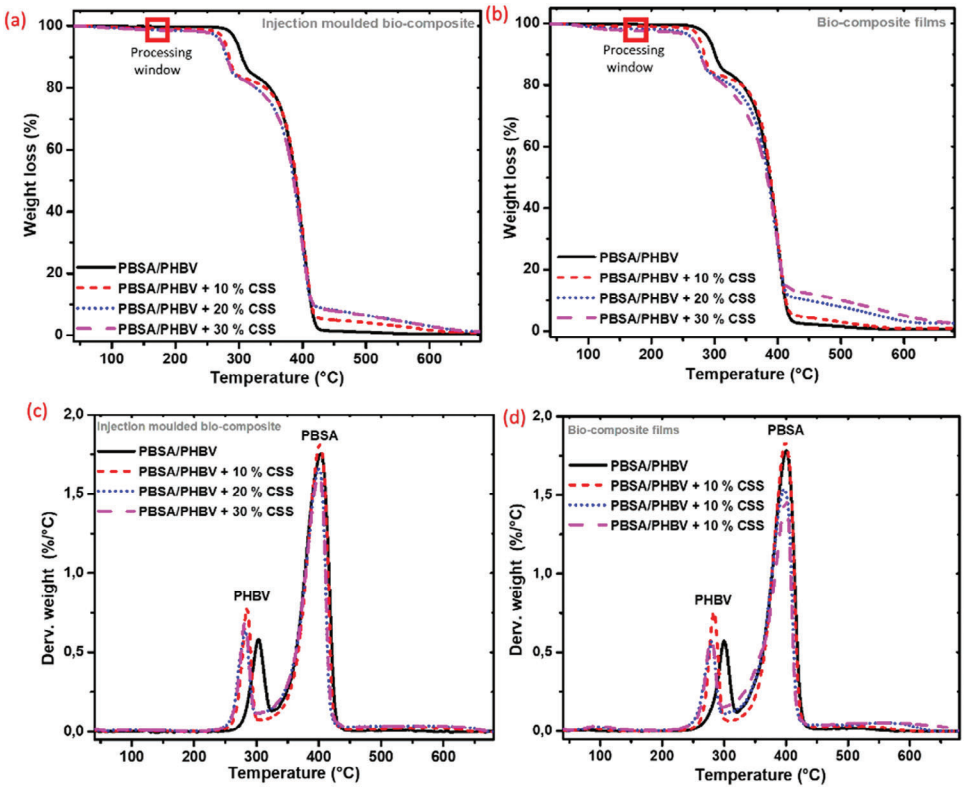

Figure 2. TGA curves showing thermal properties of a) injection molded bio-composites. b) Bio-composite films and dTGA curves showing c) injection molded bio-composites, and d) bio-composite films containing 10%, 20%, and 30% cowpea lignocellulosic sidestream.

data, and the means were compared using Turkey's B test at $p \leq 0.05$. The independent variable was the composites containing 0%, 10%, 20%, and 30% cowpea lignocellulosic sidestream, and the dependent variables were the measured values.

3. Results and Discussion

3.1. Thermal and Thermomechanical Properties of Injection Molded Bio-Composites and Bio-Composite Films

The Thermogravimetric analysis (TGA) and derivative TGA (dTGA) of injection molded bio-composites and bio-composite films depict the effect of the fibers on the thermal stability of the polymers. The TGA curves and dTGA curves of injection molded and bio-composite films are shown in **Figure 2**, and the detailed results, such as initial degradation temperature (T_o), maximum degradation temperature (T_{max1} and T_{max2}) and residue at 600 °C are shown in Tables S1 and S2 (Supporting Information). The thermal stability of pure PBSA, PHBV, and the cowpea lignocellulosic fibers are shown in Figure S1 (Supporting Information). The PBSA/PHBV blend (injection molded and films) had a T_o of 287 and 283 °C, respectively. The T_o decreased with fiber addition for both injection molded and bio-composite films, with the bio-composites containing 30% fibers showing the largest decrease of 30 °C relative to the PBSA/PHBV blend. Fiber loading up to 30% reduces the relative amounts of PBSA and PHBV, thus since the fibers have a lower onset degradation temperature compared to PBSA and PHBV (Figure S1, Supporting Information), their addition decreased the overall thermal stability of bio-composites containing fibers.

All samples displayed a two-stage degradation pattern, as observed by two peak degradation temperatures (T_{max}) from the dTGA curves (Figure 1c,d). T_{max1} corresponds to PHBV, whereas T_{max2} corresponds to PBSA. In both the injection molded and bio-composite films, PBSA displayed a T_{max} around 400 °C, which was unaffected by the addition of the fibers (Figure 2a,b). In contrast, the T_{max} of PHBV occurred around 300 °C and decreased in both injection molded and bio-composite films with the addition of the fibers. At 30% fiber loading, T_{max2} of PHBV decreased by 19 and 25 °C in injection molded bio-composites and bio-composite films, respectively. This suggests that the thermal stability of PBSA was unaffected by fiber addition, whereas the thermal stability of PHBV decreased with fiber addition.

The thermal degradation mechanism of PHBV involves a random scission process induced by the β-hydrogen elimination process (six-membered ring ester decomposition process), giving rise to crotonic acid and croton end-group chains as degradation products; this reduces the polymer molecular weight.[21–23] Whereas, the thermal degradation mechanism of PBSA also involves the β-hydrogen scission or β-decomposition of the polymeric backbone.[24] The cowpea lignocellulosic fibers had a T_o of 263 °C (Figure S1, Supporting Information), which is below the T_o of the PBSA/PHBV blend and the T_{max} of PHBV. Mazur et al.[14] Showed that PHBV and agricultural fibers displayed a one-step degradation pattern. Since the fibers start to degrade

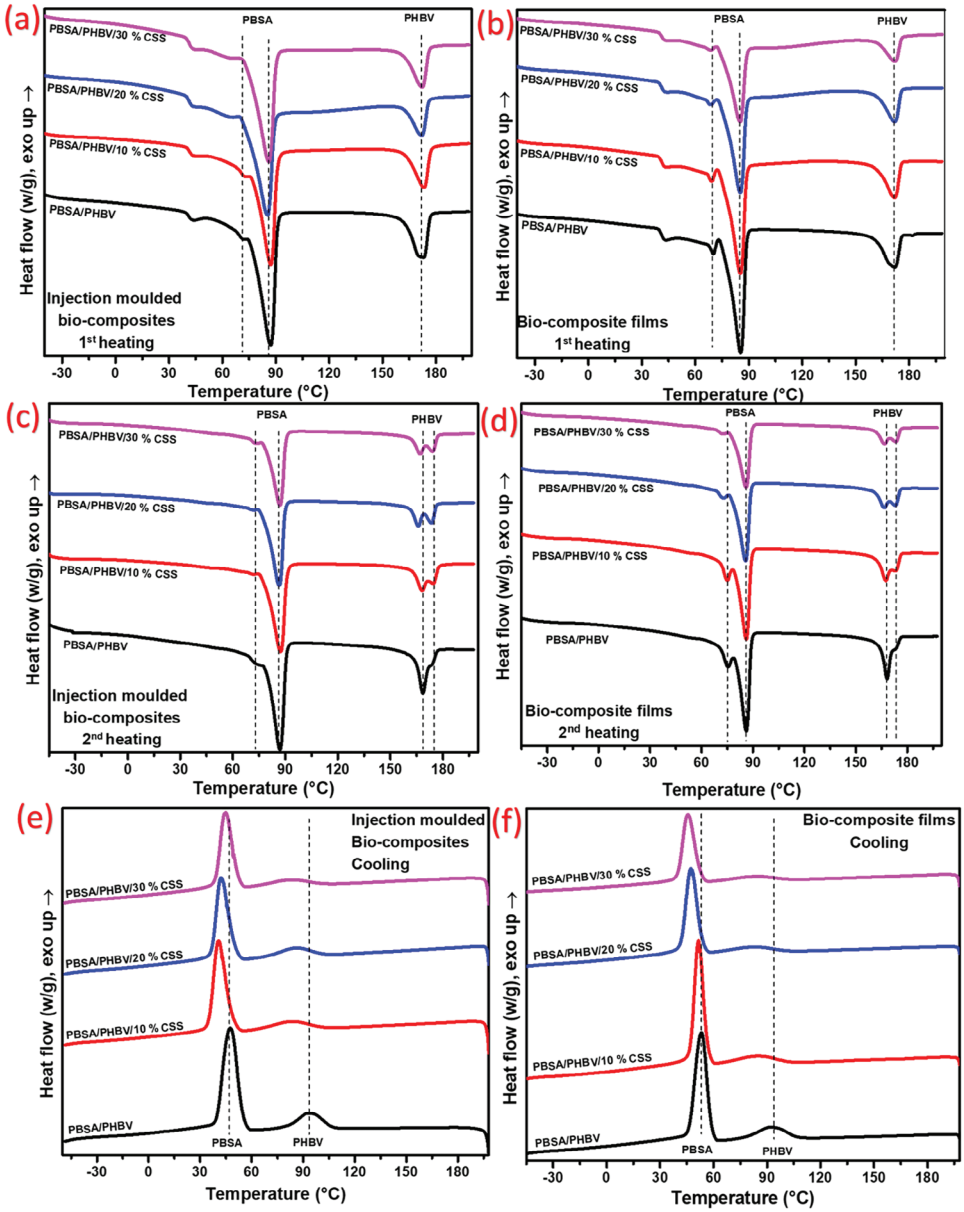

Figure 3. DSC curves showing 1st and 2nd heating curves of a,c) injection molded and b,d) bio-composite films, and cooling curves of e) injection molded and f) bio-composite films containing 10%, 20%, and 30% cowpea lignocellulosic sidestream.

before PHBV, the degradation products of the cowpea fibers, such as acetic acid produced during hemicellulose degradation, may promote random chain scission of PHBV to decrease the thermal stability.[25] PBSA, on the other hand, has a T_{max} that is 147 °C higher than the T_o of cowpea fibers and 62 °C higher than the T_{max} of cowpea fibers. Therefore, around 400 °C (T_{max} of PBSA), most of the hemicellulose and cellulose and intermediate degradation products would have been converted to biochar, thus not affecting the T_{max} of PBSA.

The melting temperatures from the first and second heating curve (T_m), melt crystallization temperatures (T_c) of PBSA and PHBV in injection molded and bio-composite films are shown in **Figure 3**. The detailed results from DSC, that is T_m, T_c, and crystallinity (X_c) of PBSA and PHBV in the injection molded and bio-composite films are shown in Tables S1 and S2 (Supporting Information), respectively.

The PBSA/PHBV blend (injection molded and film) displayed two major melting events corresponding to PBSA and PHBV, respectively (Figure 3a–d). From both the first heating and second heating curves (Figure 3a–d), PBSA displayed a double melting peaks, which have been widely reported elsewhere.[26–28] In contrast, PHBV only displayed one peak during first heating (Figure 3b) and double melting peaks during the second heating. The double melting peaks may be ascribed to the melt crystallization behavior during the heating process. In the first step, the melting and recrystallization of low-melting crystals with lower thermal stability occur, followed by the melting of crystals with higher thermal stability formed through recrystallization.

Multiple melting phenomena can also be ascribed to different crystal lamella formations, resulting in heterogeneous crystal morphology.[27]

The minor melting peak (T_{m1}) of PBSA in both injection molded and bio-composite films shifted to a lower temperature and decreased in intensity with fiber addition, possibly due to the restriction of polymer chain mobility by the filler[27] while the major melting peak (T_{m2}) was unaffected as observed from the first and second heating curves (Figure 3a–d). This shows that fiber addition resulted in a more homogeneous crystal morphology of PBSA in both injection molded and bio-composite films. PHBV on the other hand displayed one peak in the PBSA/PHBV blend (injection molded and bio-composite film) in the first heating curve and double melting peaks in the second heating curve. From the first heating curve, fiber addition did not affect the melting temperature of PHBV. However, in the second heating curve, the major peak of PHBV (T_{m1}) decreased in intensity, while the minor melting peak (T_{m2}) increased in intensity, resulting in two intense peaks. In other words, fiber addition resulted in more heterogeneous crystal morphology (Figure 3a,b) of PHBV.

In previous studies, it was reported that an improvement in interfacial adhesion between PBSA and hop fibers resulted in more homogeneous crystal morphology, whereas, poor interfacial resulted in enhanced heterogeneous crystal morphology.[26] Rodriguez-Uribe et al.[8] also reported that stronger interactions between the filler (talc) and polymer (BioPBSA/maleic anhydride grafted PBSA) resulted in more homogeneous crystal morphology. Based on literature studies, herein, the more homogeneous crystal morphology of PBSA and more heterogeneous crystal morphology of PHBV with fiber addition may suggest that the fibers have a better affinity to PBSA than PHBV.

The PBSA/PHBV blend (injection molded and films) displayed two melt crystallization peaks (T_c) during cooling, corresponding to PHBV and PBSA (Figure 3e,f). The T_c of both PSBA and PHBV decreased with fiber addition for both injection molded (Figure 3e) and bio-composite films (Figure 3f) relative to the neat PBSA/PHBV blends. However, PHBV displayed a greater decrease in T_c compared to PBSA upon fiber addition. The decrease in T_c could be due to the dispersed fibers hindering the chain mobility of PBSA and PHBV, thus delaying nucleation of polymer crystallization. The larger decrease in the T_c of PHBV suggests that PHBV chains were more restricted toward nucleation than PBSA. This may be because PHBV is the most crystalline material in the composite and needs more time during cooling to reorganize and form the crystals compared to PBSA. A decrease in T_c with fiber addition has been reported for polymers filled with natural fibers, such as bamboo fibers,[29] coffee silverskin,[30] and mixed faba bean stems and pods.[15]

The effect of the fibers on the crystallinity of both PBSA and PHBV in the bio-composites was investigated, considering the weight fraction of the fibers, and the results are in Tables S1 and S2 (Supporting Information). In the PBSA/PHBV blend (injection molded and film), PBSA had a crystallinity of 45% and 50%, respectively, whereas PHBV had a crystallinity of 56% and 65%, respectively. These values are similar to those reported in other studies, where PBSA had a crystallinity of 43%, while PHBV had a crystallinity of 67% in PBSA/PHBV blends (70/30).[12] The crystallinity of PBSA and PHBV decreased with fiber addition in both the injection molded bio-composites and bio-composite films. The decrease in crystallinity of PBSA and PHBV is due to restricted chain mobility of polymer segments toward nucleation by the fibers, as reported elsewhere for polymers filled with natural fibers, such as cellulose fibers,[31] and wheat straw fibers.[32]

The storage modulus (E') and maximum tan δ (**Figure 4**) give important information about thermodynamically favorable interactions between a polymer matrix and the reinforcing fibers.[33] The E' of all samples decreased with an increase in temperature, indicating the softening of the material, an intrinsic property of thermoplastic polymers (Figure 4a,b). The E' of both injection molded and bio-composite films increased with an increase in fiber loading over the entire temperature range (−70–60 °C) due to the restriction of polymer chain movement by the fibers. This suggests that the fibers were effective as a reinforcing filler, increasing the overall stiffness of the injection molded and bio-composite films compared to the PBSA/PHBV blend without the fibers.

The maximum tan δ can be considered as the glass transition temperature (T_g) of polymers. Two distinct T_g's were observed for injection molded (Figure 4c) and bio-composite films (Figure 4d), indicating that PBSA and PHBV are thermodynamically immiscible as reported elsewhere for PHBV/PBSA blends at varying PBSA ratio.[12,34] In the injection molded PBSA/PHBV blend, PBSA and PHBV displayed T_g's at −36.58 and 6.08 °C (Figure 4c), respectively, which were slightly lower in the bio-composite films at −39.69 and 0.76 °C (Figure 4d), respectively. In the injection molded bio-composites, the T_g of both PBSA and PHBV increased to higher temperatures with fiber addition due to the restriction of molecular chain mobility of polymers by the fibers.[35] In contrast, in the bio-composite films, the T_g's of both PBSA and PHBV did not shift to higher temperatures with fiber addition.

Tan delta is the mechanical dampening factor defined as a ratio of loss modulus and storage modulus. The height of the tan delta at T_g is an important parameter that indicates dampening. Generally, a composite with good matrix/fiber interfacial adhesion dissipates less energy as there is reduced molecular chain mobility at the fiber/matrix interface, resulting in a decrease in tan delta peak at T_g. In contrast, poor matrix/fiber interfacial adhesion dissipates more energy resulting in an increase in the tan delta height at T_g.[33,35] In this work, the tan delta height at T_g of PBSA decreased with fiber addition, dissipating less energy. In contrast, the tan delta height at T_g of PHBV increased with fiber loading, dissipating more energy. This suggests that the PBSA matrix/fiber interfacial adhesion was better than the PHBV matrix/fiber interfacial adhesion. This trend was observed for both injection molded (Figure 4c) and bio-composite films (Figure 4d).

Two trends were notable from DSC and DMA results. That is, homogeneous crystal morphology associated with good interfacial adhesion was observed for PBSA, whereas heterogeneous crystal morphology associated with poor interfacial adhesion was observed for PHBV, as discussed earlier. In addition, a decrease in dampening associated with good interfacial adhesion was observed for PBSA, whereas an increase in dampening associated with poor interfacial adhesion was observed for PHBV. These trends suggest that the fibers had more affinity to PBSA than PHBV and can be explained by thermodynamic and kinetic factors, which are known to affect the affinity of a filler in a polymer blend system.[36] If one considers the kinetic factors, PBSA has

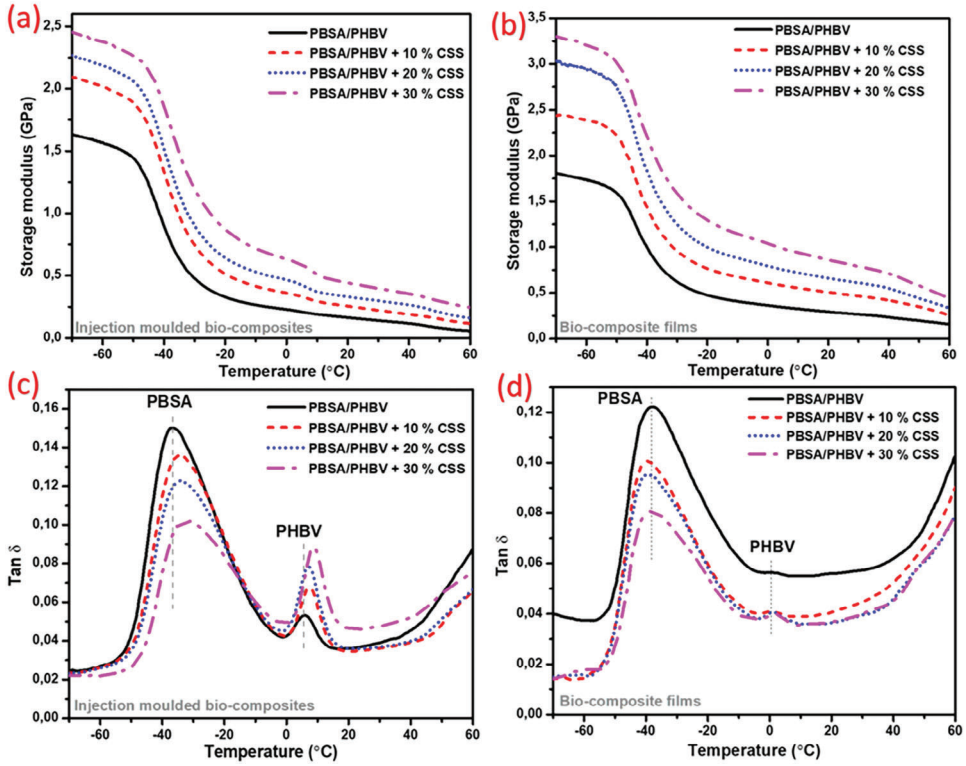

Figure 4. DMA curves showing storage modulus versus temperature of a) injection molded bio-composites. b) Bio-composite films and tan delta versus temperature of c) injection molded bio-composites and d) bio-composite films containing 10%, 20%, and 30% cowpea sidestream.

a lower melting point and lower viscosity compared to PHBV.[12] In polymer blends, a polymer with lower viscosity PBSA in this case, has a better wetting coefficient than PHBV, making it easier for the filler to diffuse into it, leading to good interfacial adhesion. If one considers the thermodynamic factors, PBSA has higher water wettability, indicated by a lower contact angle of 68° and has more polar components compared to PHBV, which has a higher contact angle of 76° and fewer polar components.[11] Therefore, the hydrophilic cowpea lignocellulosic fibers are expected to have more affinity and adhesion to PBSA than PHBV, as discussed.

3.2. Freeze-Fractured Morphology of Injection Molded and Bio-Composite Films

The freeze-fractured morphology of injection molded and bio-composite films are highlighted in **Figure 5**. The injection molded PBSA/PHBV blend (Figure 5a) displayed a co-continuous morphology, where the PBSA and PHBV phases cannot be discriminated at the micron scale. The PBSA/PHBV blend produced by extrusion film cast (Figure 5e) also displayed co-continuous morphology with the fibrous-like alignment of polymer segments in the processing direction. This is due to the stretching of the polymer chain segments by the chill rolls as the film exits the die during film cast extrusion.[37,38] In addition, the oriented polymer segments may act as crystal nucleation points to induce crystallization before the polymer cools down and solidifies in the chill rolls.[39] This may have resulted in higher crystallinity of PBSA and PHBV in extrusion cast films than injection molding.

The morphology of the injection molded bio-composite containing 10% (Figure 5b) and 20% fibers (Figure 5c) suggest good interfacial adhesion between the fibers and the polymer matrix (shown by arrows) with no significant gap between the matrix and the fibers. The morphology injection molded bio-composite containing 30% fibers (Figure 5d) showed limited interfacial gap between the polymers and the fibers. The bio-composite film containing 10% (Figure 5f), 20% (Figure 5g), and 30% fibers (Figure 5h) also suggest good interfacial adhesion between the polymer matrix and the fibers (shown by arrows), with no gap at the polymer matrix/fiber interface. Other studies have reported good interfacial adhesion in natural fiber-reinforced polymers For example, Harder et al.[26] reported good interfacial adhesion between PBSA and natural hop fibers (1 mm length) with the absence of interfacial gap. Meanwhile, Ahankari et al.[40] reported good interfacial adhesion between PHBV and corn straw fibers.

In both injection molded and bio-composite films, some voids (shown by dotted circles) can be observed in the images (Figure 5). More voids can be seen in the bio-composite films compared to injection molded bio-composites due to differences in processing. During injection molding, the filling of the mold is under high pressure which may lead to better packing of polymer chains and the fibers, compared to film cast extrusion which involves stretching of the films as it exists the die by the chill

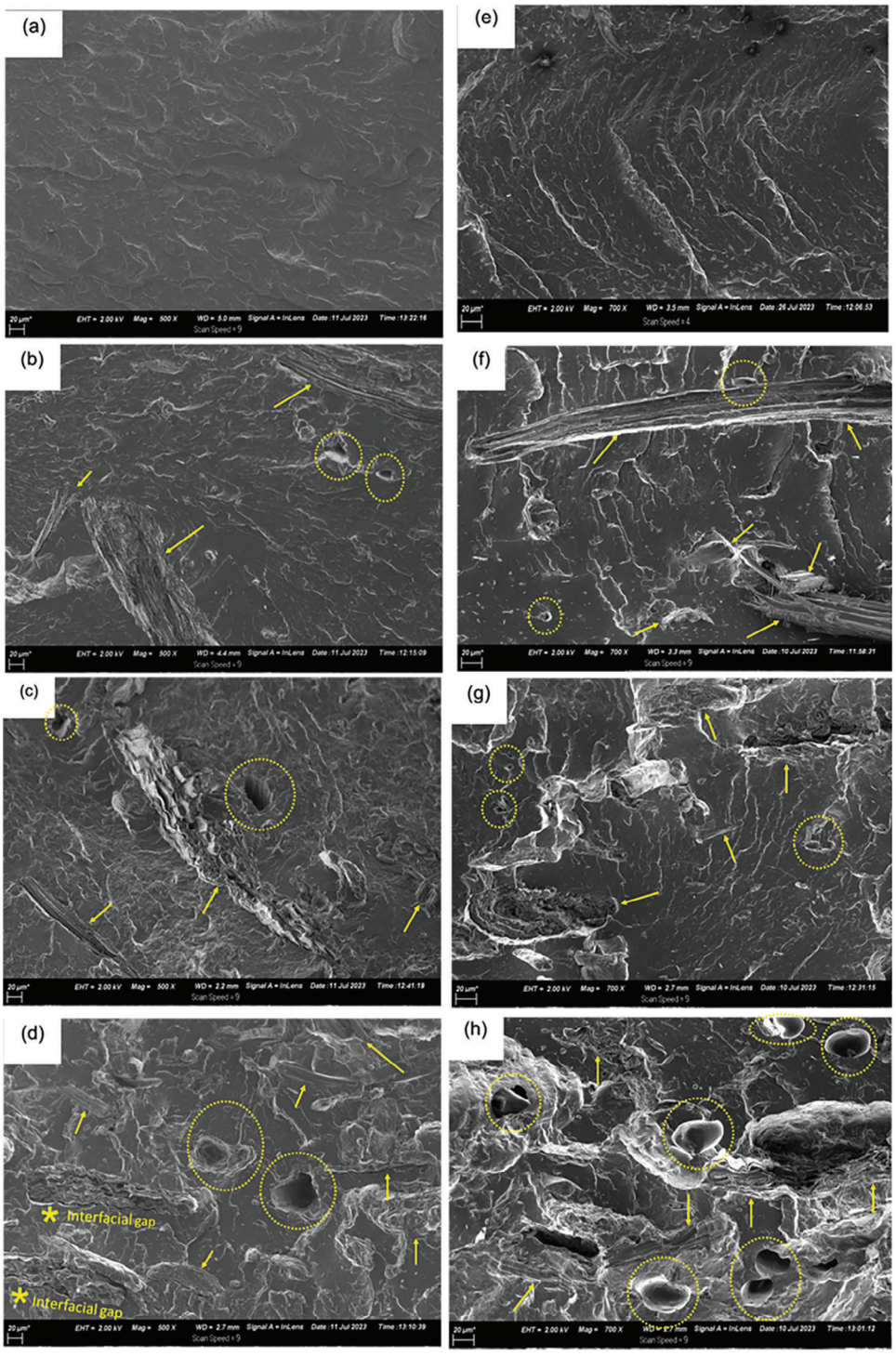

Figure 5. Freeze-fractured SEM morphology of injection molded a) PBSA/PHBV blend with b) 10%, c) 20%, and d) 30% cowpea lignocellulosic fibers. The PBSA/PHBV bio-composite films e) with f) 10%, g) 20%, and h) 30% cowpea lignocellulosic fibers.

rolls. Therefore, better packing and compaction during injection molding may lead to lower porosity compared to bio-composite films. Pal et al.[37] also reported that compression molding under pressure enhanced packing density compared to film cast extrusion.

3.3. X-Ray Tomography

The alignment of the fibers in the polymer matrix was investigated by 3D X-ray tomography, and the reconstructed slice images of injection molded bio-composites and bio-composite films

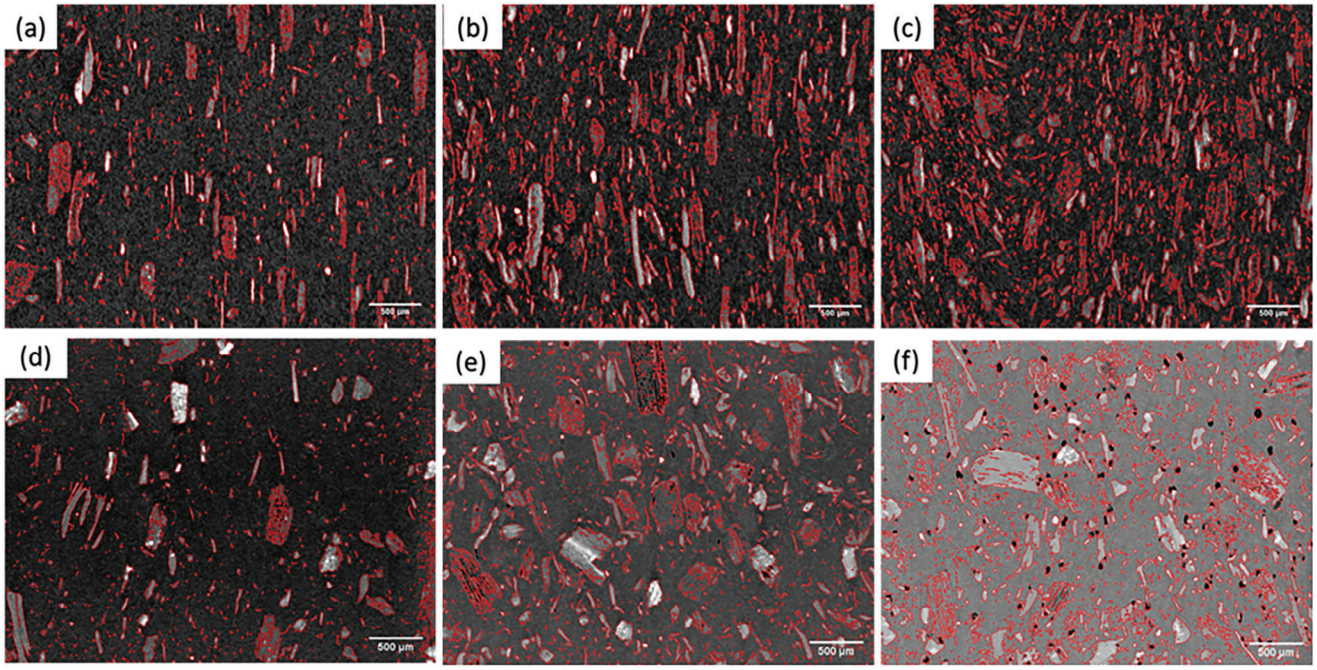

Figure 6. X-ray tomography slice images of injection molded bio-composites containing a) 10%, b) 20%, and c) 30% cowpea lignocellulosic sidestream, and bio-composite films containing d) 10%, e) 20%, and f) 30% cowpea lignocellulosic sidestream. Red pseudocolor highlights the edges of the fiber material.

are shown in **Figure 6**. The red pseudocolor highlights the edges of the light gray cowpea lignocellulosic fibers, while the darker background indicates the PBSA/PHBV matrix, and the black spots (visible only in Figure 6e,f) depicts pores/voids. The injection molded bio-composites containing 10% (Figure 6a), 20% (Figure 6b), and 30% fibers (Figure 6c) showed unidirectional alignment of the fibers within the polymer matrix in the inflow mold direction. Similarly, the bio-composite films containing 10% (Figure 6d), 20% (Figure 6e), and 30% fibers (Figure 6f) also showed unidirectional alignment of the fibers in the inflow direction. However, the fibers seemed to be better unidirectionally aligned in the injection molded bio-composites than in the bio-composite films. Fiber dispersion and orientation are influenced by processing parameters, such as pressure, temperature, and mixing processes.[41] During injection molding, the filling of the mold occurs under high pressure, followed by quick cooling of the mold; this may lead to better packing and alignment of the fibers within the polymer matrix. In contrast, during film cast extrusion, the film is being stretched by the chill rolls while it is being cooled slowly.

The X-ray tomography images of the injection molded bio-composites and bio-composite films (see visualizations: Figure 6; and Figures S2 and S4, Supporting Information) were used to calculate the volume fraction of pores/voids and the results are shown in **Figure 7**. The occurrence of voids/pores are unavoidable in fiber-reinforced polymers and affect their mechanical properties.[41] The injection molded bio-composite containing 10%, 20%, and 30% fibers had 0.03%, 0.2%, and 0.6% pores, respectively. Meanwhile, the bio-composite films containing 10%, 20%, and 30% cowpea fibers had 1%, 1%, and 4% pores. Generally, pores in natural fiber-reinforced polymers are a function of fiber loading; hence, the volume fraction of pores increased with fiber loading in both injection molded and bio-composite films.[42] There are several sources of the pores in natural fiber-reinforced polymers; they may be due to the pores in the fibers (lumen), some entrapped air and humidity during processing, fiber/matrix interface pores due to poor wetting of the fibers by matrix, and limited compaction of the fibers and polymer matrix.[41,43,44] As explained earlier, the lower volume fraction of pores/voids in injection molded bio-composites compared to bio-composite films may be due to better packing and compaction during injection molding.

The diameter of the pores for both the injection molded and bio-composite films is shown in Figure 7c,d, respectively. The injection molded bio-composite containing 10% cowpea lignocellulosic sidestream had an average pore diameter of about 110 µm and decreased to 90 and 70 µm with the addition of 20% and 30% cowpea lignocellulosic fibers. In contrast, the bio-composite film containing 10% pores had an average pore diameter of 10 µm that increased to 12 and 17 µm with fiber loading.

3.4. Tensile Properties of Injection Molded Bio-Composites and Bio-Composite Films

The tensile properties of injection molded bio-composites and bio-composite films are shown in **Figure 8**. The tensile strength of fiber reinforced polymers depends on various factors, such as fiber orientation, length, and interfacial adhesion between the polymer and fibers.[45]

The injection molded PBSA/PHBV blend had a tensile strength of 17.46 MPa, which increased with fiber loading

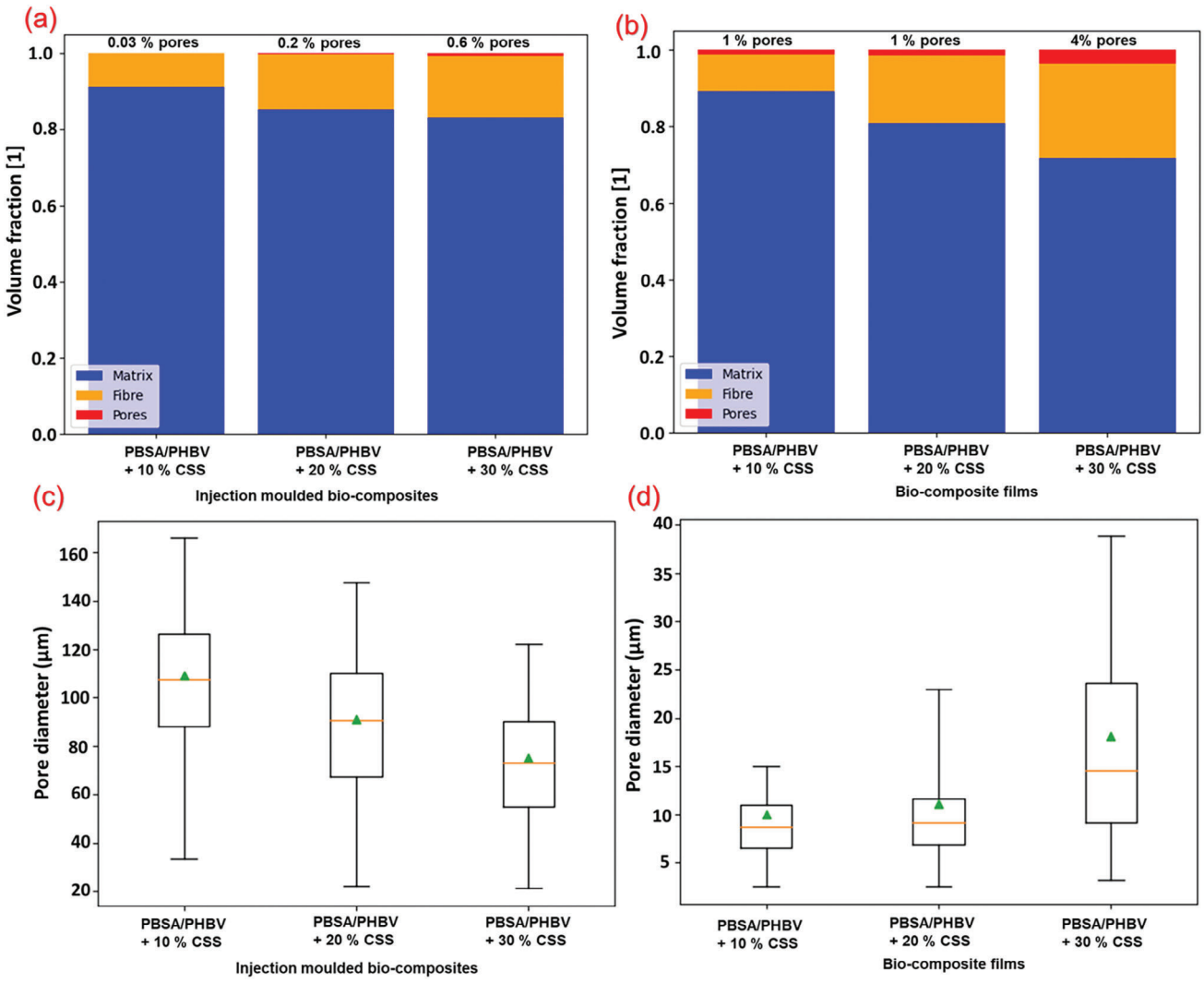

Figure 7. Volume fractions of the PBSA/PHBV matrix, fibers, and pores in a) injection molded bio-composites, and b) bio-composite films. Box and Whisker plot shows the pore diameter of c) injection molded and d) bio-composite films. In the box and whisker plot, the green triangle and orange lines are means and median of pore diameter, respectively.

(Figure 8a). The increase in tensile strength with fiber addition is an indication of good interfacial adhesion between a polymer matrix and fibers, as previously shown by SEM (Figure 5), for efficient stress transfer when load is applied. Generally, at higher fiber loading, the stress can be transferred to more fibers, and the matrix can carry the load after fiber fractures to increase the tensile strength.[46] In the previous section (Figure 6), it was shown that the fibers were unidirectionally aligned in the inflow mold direction. This might have also increased the tensile strength with fiber loading, as the unidirectionally aligned fibers in the inflow mold direction have a tendency to exhibit buckling in the composite, leading to higher tensile strength.[47]

The effect of fiber loading on the tensile strength of bio-composite films (Figure 8d) was different from the injection molded bio-composites (Figure 8a). Contrary to injection molded bio-composites, which showed an increase in tensile strength with fiber addition, the addition of 10%, 20%, and 30% fibers decreased the tensile strength from 18.8 MPa in the PBSA/PHBV blend films to about 10 MPa (Figure 8d). This is despite SEM showing good interfacial adhesion between the polymer matrix and the fibers (Figure 5). The decrease in tensile strength in the bio-composite films may be related to the occurrence of pores/voids. In the previous section, it was demonstrated that an increase in fiber loading resulted in large volume fraction of pores in bio-composite films (Figure 7), which may act as stress raisers when load is applied to decrease tensile strength. Judd [48] demonstrated that regardless of polymer matrix and fiber type, the shear strength of composites decreased by 7% for each 1% void.

The Young's modulus of both injection molded (Figure 8b) and bio-composite films (Figure 8e) increased with an increase in fiber loading as expected. Unlike tensile strength, which is dependent on matrix/fiber interfacial adhesion, Young's modulus is a linear function of fiber loading and is related to the stiffness of the fibers.[14] Since lignocellulosic fibers have higher stiffness compared to the polymer matrix, fiber loading leads to an

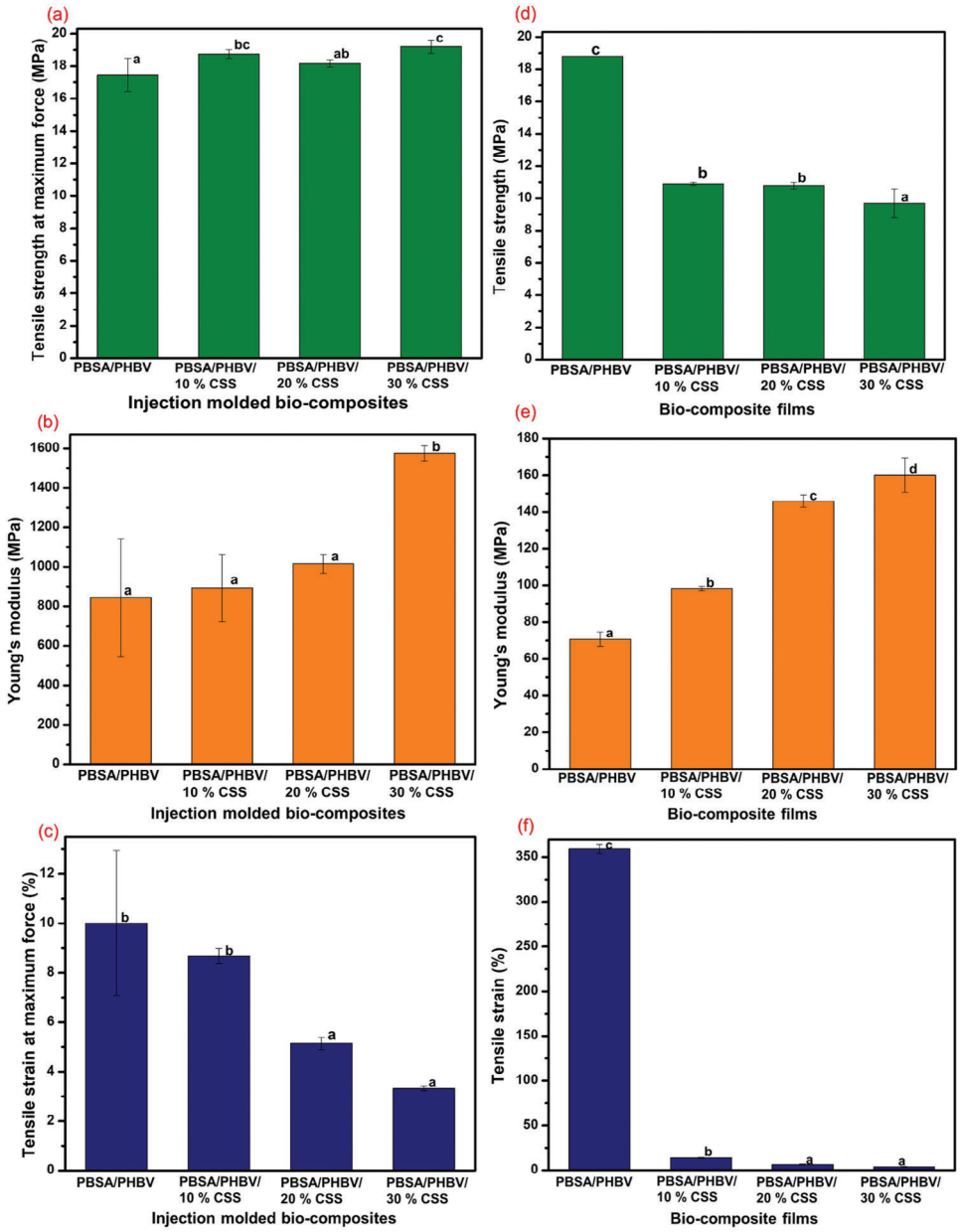

Figure 8. Tensile properties of injection molded bio-composites and bio-composite films. The bars with different letters are statistically significant at $p < 0.05$.

increase in Young's modulus/stiffness of the bio-composites.[49] The increase in stiffness of the bio-composites with fiber loading was also demonstrated by an increase in storage modulus (Figure 4a,b). The lower Young's modulus of bio-composite films compared to injection molded bio-composite at similar fiber loading may be related to decreased sample thickness as reported elsewhere for injection molded PBS/polyglycolic acid (PGA) blend and film blown PBS/PGA blend.[50]

The tensile strain of both injection molded (Figure 8c) and bio-composite films (Figure 8f) decreased with an increase in fiber loading. The fracture dynamics of polymers reinforced with short fibers were studied in detail, and the alignment of the fibers was found to influence crack propagation.[47,51] The X-ray tomography images showed that the fibers were unidirectionally aligned in the processing direction (Figure 6). When the fibers are aligned in the processing direction, the microfailure starts at the fiber tips and propagates near fiber ends within the polymer matrix in a zigzag manner perpendicular to the load direction as the fibers do not stretch under load due to their high stiffness.[47,51] Therefore, an increase in fiber loading results in higher initiation points of microfailure near fiber tips and ease of crack propagation between fibers, leading to a decrease in tensile strain. In addition, an increase in fiber loading decreased the volume fraction of polymer available for elongation. While the alignment of fibers in the process direction increases tensile strength, it decreases tensile strain compared

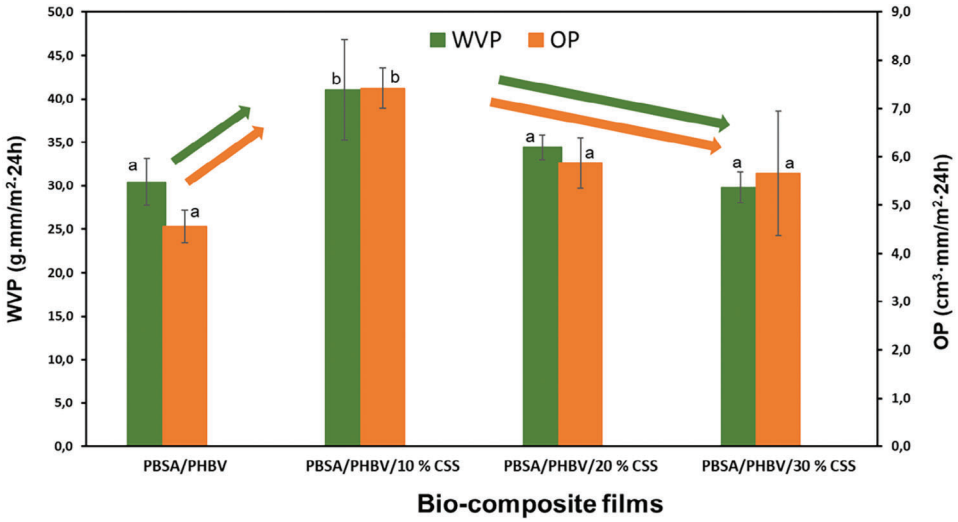

Figure 9. Water vapor permeability and oxygen permeability of bio-composite films containing 10%, 20%, and 30% cowpea lignocellulosic sidestream. Bars with the same color that have different letters are statistically significant at $p < 0.05$.

to fibers aligned at an angle or perpendicular to the processing direction.[47]

3.5. Water Vapor Permeability and Oxygen Permeability

The water vapor permeability (WVP) and oxygen permeability (OP) of the bio-composite films were investigated, and the results are shown in **Figure 9**. The PBSA/PHBV bio-composite film had a WVP and OP 30.44 g mm m^{-2}, 24 h and 4.56 cm^3 mm m^{-2}, 24 h, respectively. The addition of 10% fibers increased WVP and OP to 41.01 g mm m^{-2}, 24 h and 7.42 cm^3 mm m^{-2} 24 h, respectively. It is well-documented that the diffusion of water molecules and oxygen occurs through the amorphous phase of a polymer.[8] The DSC results earlier showed that fiber addition decreased the crystallinity of both PBSA and PHBV. Therefore, the increase in WVP and OP with fiber addition can be attributed to the decrease in the crystallinity of the polymer matrix and an increase in hydrophilic fiber.

The OP and WVP decreased with the addition of 20% and 30% fibers relative to the bio-composite film containing 10% fibers. However, there was no statistical significance in the OP and WVP of the PBSA/PHBV blend film and bio-composite containing 20% and 30% fibers, even though the crystallinity decreased linearly with fiber addition. A similar trend was observed for HDPE reinforced with cellulose fibers.[52] These authors reported that above 10% fiber loading, the blocking effect of cellulose fibers is more significant than the crystallinity of the polymer matrix in decreasing the diffusion, thus permeation of gases and water vapor. Lignocellulosic fibers contain semicrystalline cellulose, and these crystals in cellulose are considered impenetrable to water vapor and gases.[53] Therefore, the cellulose crystals in the unidirectionally aligned lignocellulosic fibers may possibly reduce the diffusion of the permeants (water vapor and oxygen) through the film thickness by creating a tortuous pathway. Thus, the decrease in OP and WVP in bio-composites containing 20% and 30% fibers compared to the bio-composite containing 10% fibers might be due to the blocking effect of the fibers at higher volume fraction by creating more tortuous pathways.

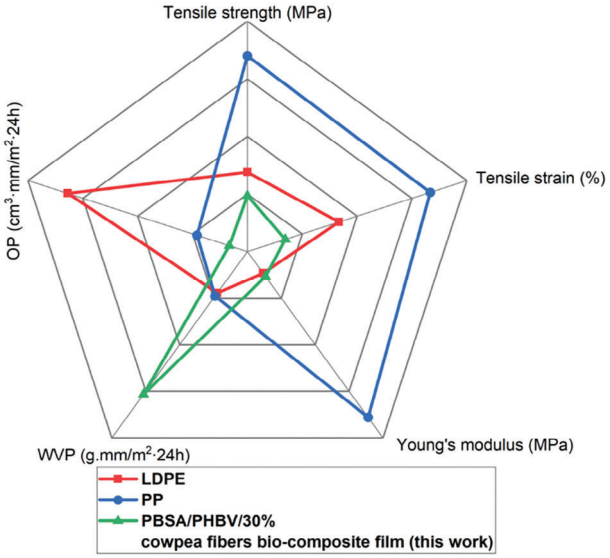

Figure 10. Performance (mechanical and barrier properties) of bio-composite film containing 30% cowpea fibers compared to conventional polymers LDPE and PP.

The performance of the developed bio-composite films can be compared to commercial synthetic polymers, such as low-density polyethylene (LDPE) and polypropylene (PP).[54] For comparison, the bio-composite film containing 30% cowpea fibers will be compared to LDPE and PP films as shown in **Figure 10**. The bio-composite film in this study had significantly lower tensile strength and strain compared to PP and LDPE films. However, the Young's modulus (stiffness) was comparable to that of LDPE, but significantly lower than that of PP. In terms of barrier properties, compared to PP and LDPE films, the developed bio-composite films (PBSA/PHBV/30% cowpea fibers) had poor

water vapor permeability, but better oxygen permeability. Thus, in general, although the developed bio-composite films had inferior overall tensile properties compared to PP and LDPE films, its lower oxygen permeability may be attractive in packaging applications where lower oxygen permeability is desired. In addition, the developed bio-composite films are fully bio-based, and biodegradable compared to synthetic conventional PP and LDPE which are not biodegradable.

The cost effectiveness of the developed bio-composite materials can be compared to synthetic conventional polymers, such as LDPE and PP. The pristine LDPE and PP cost less than 2.0 € kg^{-1},[55] whereas biodegradable polymers cost more than 2 times the price of conventional polymers, depending on various factors. For example, PBSA costs ranges around 3 € kg^{-1}, with PHBV costing between 3 and 5 € kg^{-1}.[56] The pristine PBSA/PHBV blend (ratio 85/15) would have an estimated cost of around 3.2 € kg^{-1}. Thus, the addition of 30% low value cowpea fibers will potentially reduce the price of the developed materials. In general, while the developed bio-composites have an estimated cost higher than that of commercially available PP and LDPE films, the growing restriction of conventional petroleum-based polymers, and the growing demand for more sustainable biodegradable packaging materials may reduce the cost of production of these bio-composites in the future so that they become cost effective compared to conventional polymers.

4. Conclusions

In this work, cowpea lignocellulosic fibers were demonstrated as a filler in a PBSA/PHBV blend matrix to produce injection molded and bio-composite films for application in rigid and flexible packaging, respectively. TGA, DSC, and DMA revealed that the addition of fibers affected the thermal properties of both PBSA and PHBV. The fibers were unidirectionally aligned in the processing direction and there was good interfacial adhesion between the fibers and polymer matrix as revealed by X-ray tomography and SEM, respectively. This resulted in an increase in tensile strength of injection molded bio-composites with fiber addition, meanwhile, the tensile strength of bio-composite films decreased with fiber addition. This was attributed to the differences in the two processing techniques. Bio-composite films had a higher volume fraction of pores, which may act as stress raisers when under load to decrease tensile strength. Cowpea lignocellulosic fibers were effective as reinforcing fillers, as revealed by an increase in storage and Young's modulus of both injection molded and bio-composite films. The oxygen and water vapor permeability properties of the bio-composite films containing 20% and 30% fibers were not significantly different from the PBSA/PHBV blend without the fibers. In conclusion, biodegradable bio-composite films and injection molded bio-composites were produced using bio-based biodegradable polymers and low-value cowpea lignocellulosic fibers as a filler by already existing polymer processing equipment.

Supporting Information

Supporting Information is available from the Wiley Online Library or from the author.

Acknowledgements

This work received funding from the National Research Foundation of South Africa (Grant No. MND200622534882), the European Union's Horizon 2020 research and innovation program under Grant Agreement No. 862170, and DSI/NRF Centre of Excellence in Food Security Grant ID No. 91490. The authors would like to thank Mr. Thean Geldenhuys for the supply of the cowpea sidestream from a farm in the North West Province, South Africa.

Conflict of Interest

The authors declare no conflict of interest.

Author Contributions

M.A.M.: Conceptualization, Methodology, Formal Analysis, Investigation, Software, Writing – Original Draft, Writing – Review & Editing. A.T.: Conceptualization, Methodology, Writing – Review & Editing. E. L.: Conceptualization, Methodology, Writing – Review & Editing, J.V.: Formal Analysis, N.S.: Formal Analysis, Resources, Writing – Review & Editing. M.S.: Resources, Writing – Review & Editing. S.S.R.: Resources, Writing – Review & Editing, Supervision. J.K.: Conceptualization, Resources, Writing – Review & Editing, Supervision, Project administration. M.N.E.: Conceptualization, Validation, Resources, Writing – Review & Editing, Main Supervision.

Data Availability Statement

The data that support the findings of this study are available from the corresponding author upon reasonable request.

Keywords

bio-composites, cowpea fibers, films, injection molded, lignocellulose, packaging, sidestream

Received: February 1, 2024
Revised: March 12, 2024
Published online:

[1] F. Zhang, Y. Zhao, D. Wang, M. Yan, J. Zhang, P. Zhang, T. Ding, L. Chen, C. Chen, *Clean. Prod.* **2021**, *282*, 124523.
[2] R. Geyer, J. R. Jambeck, K. L. Law, *Sci. Adv.* **2017**, *3*, e1700782.
[3] R. Mori, *RSC Sustainability* **2023**, *1*, 179.
[4] M. S.-L. Yee, L.-W. Hii, C. K. Looi, W.-M. Lim, S.-F. Wong, Y.-Y. Kok, B.-K. Tan, C.-Y. Wong, C.-O. Leong, *Nanomaterials* **2021**, *11*, 496.
[5] A. Mtibe, M. P. Motloung, J. Bandyopadhyay, S. S. Ray, *Macromol. Rapid Commun.* **2021**, *42*, 2100130.
[6] J. Xu, B. H. Guo, *Biotechnol. J.* **2010**, *5*, 1149.
[7] L. Meng, L. Yu, S. Khalid, H. Liu, S. Zhang, Q. Duan, L. Chen, *Composites, Part B* **2019**, *177*, 107384.
[8] A. Rodriguez-Uribe, T. Wang, A. K. Pal, F. Wu, A. K. Mohanty, M. Misra, *Composites, Part C* **2021**, *6*, 100201.
[9] F. Yang, C.-L. Zhang, Y. Han, Z.-R. Ma, Y.-X. Weng, *Chin. J. Polm. Sci.* **2023**, *41*, 1805.
[10] P. Kamrit, M. Seadan, S. Suttiruengwong, *Suan Sunandha Sci. Tech. J.* **2022**, *9*, 22.
[11] M. Salomez, M. George, P. Fabre, F. Touchaleaume, G. Cesar, A. Lajarrige, E. Gastaldi, *Polym. Degrad. Stab.* **2019**, *167*, 102.

[12] B. L. Delliou, O. Vitrac, M. Castro, S. Bruzaud, S. Domenek, *J. Appl. Polym. Sci.* **2022**, *139*, 52124.
[13] S. Lammi, E. Gastaldi, F. Gaubiac, H. Angellier-Coussy, *Polym. Degrad. Stab.* **2019**, *166*, 325.
[14] K. E. Mazur, P. Jakubowska, A. Gaweł, S. Kuciel, *Sustainable Mater. Technol.* **2022**, *31*, e00390.
[15] M. A. Masanabo, A. Tribot, E. Luoma, N. Sharmin, M. Sivertsvik, M. N. Emmambux, J. Keränen, *Polym. Test.* **2023**, *123*, 108047.
[16] L. N. Horn, H. Shimelis, *Ann. Agric. Sci.* **2020**, *65*, 83.
[17] O. Boukar, N. Belko, S. Chamarthi, A. Togola, J. Batieno, E. Owusu, M. Haruna, S. Diallo, M. L. Umar, O. Olufajo, *Plant Breed* **2019**, *138*, 415.
[18] K. G. Satyanarayana, G. G. Arizaga, F. Wypych, *Prog.Polym. Sci.* **2009**, *34*, 982.
[19] M. Carrier, A. Loppinet-Serani, D. Denux, J.-M. Lasnier, F. Ham-Pichavant, F. Cansell, C. Aymonier, *Biomass Bioenergy* **2011**, *35*, 298.
[20] D. Templeton, T. Ehrman, *Laboratory Analytical Procedure No. 003*, National Renewable Energy Laboratory, Golden, CO **1995**.
[21] J. Mofokeng, A. Luyt, *J. Mater. Sci.* **2015**, *50*, 3812.
[22] M. R. Nanda, M. Misra, A. K. Mohanty, *Macromol. Mater. Eng.* **2011**, *296*, 719.
[23] C. Bonnenfant, N. Gontard, C. Aouf, *Polym. Test.* **2022**, *110*, 107561.
[24] K. Papadopoulou, E. Tarani, N. M. Ainali, K. Chrissafis, C. Wurzer, O. Mašek, D. N. Bikiaris, *Molecules* **2023**, *28*, 5330.
[25] P. Feijoo, A. Marín, K. Samaniego-Aguilar, E. Sánchez-Safont, J. M. Lagarón, J. Gámez-Pérez, L. Cabedo, *Polymers* **2023**, *15*, 2481.
[26] N. Harder, A. Rodriguez-Uribe, M. R. Snowdon, M. Misra, A. K. Mohanty, *Mater. Adv.* **2023**, *4*, 1502.
[27] S. S. Ray, J. Bandyopadhyay, M. Bousmina, *Polym. Degrad. Stab.* **2007**, *92*, 802.
[28] X. Wang, J. Zhou, L. Li, *Eur. Polym. J.* **2007**, *43*, 3163.
[29] S. Singh, A. K. Mohanty, T. Sugie, Y. Takai, H. Hamada, *Composites, Part A* **2008**, *39*, 875.
[30] V. Gigante, M. Seggiani, P. Cinelli, F. Signori, A. Vania, L. Navarini, G. Amato, A. Lazzeri, *Composites, Part A* **2021**, *140*, 106172.
[31] E. E. Tănase, M. E. Popa, M. Râpă, O. Popa, *Agric. Agric. Sci. Proc.* **2015**, *6*, 608.
[32] M.-A. Berthet, N. Gontard, H. Angellier-Coussy, *Compos. Sci. Technol.* **2015**, *117*, 386.
[33] N. Saba, M. Jawaid, O. Y. Alothman, M. Paridah, *Constr. Build. Mater.* **2016**, *106*, 149.
[34] B. L. Delliou, O. Vitrac, A. Benihya, P. Dole, S. Domenek, *Polym. Test.* **2023**, *124*, 108072.
[35] L. A. Pothan, Z. Oommen, S. Thomas, *Compos. Sci. Technol.* **2003**, *63*, 283.
[36] M. P. Motloung, V. Ojijo, J. Bandyopadhyay, S. S. Ray, *J. Appl. Polym. Sci.* **2020**, *137*, 48665.
[37] A. K. Pal, F. Wu, M. Misra, A. K. Mohanty, *Composites, Part B* **2020**, *198*, 108141.
[38] D. Song, K. Wang, J. Shen, L. Zhao, N. Xu, S. Pang, L. Pan, *Polymers* **2020**, *12*, 106.
[39] C. Zhou, H. Li, W. Zhang, J. Li, S. Huang, Y. Meng, J. d. Christiansen, D. Yu, Z. Wu, S. Jiang, *Polymer* **2016**, *90*, 111.
[40] S. S. Ahankari, A. K. Mohanty, M. Misra, *Compos. Sci. Technol.* **2011**, *71*, 653.
[41] A. Ramachandran, S. Mavinkere Rangappa, V. Kushvaha, A. Khan, S. Seingchin, H. N. Dhakal, *Macromol. Rapid Commun.* **2022**, *43*, 2100862.
[42] B. Madsen, H. Lilholt, *Compos. Sci. Technol.* **2003**, *63*, 1265.
[43] C. de Kergariou, A. L. Duigou, V. Popineau, V. Gager, A. Kervoelen, A. Perriman, H. Saidani-Scott, G. Allegri, T. H. Panzera, F. Scarpa, *Composites, Part A* **2021**, *141*, 106183.
[44] M. Mehdikhani, L. Gorbatikh, I. Verpoest, S. V. Lomov, *J. Compos. Mater.* **2019**, *53*, 1579.
[45] S.-Y. Fu, X.-Q. Feng, B. Lauke, Y.-W. Mai, *Composites, Part B* **2008**, *39*, 933.
[46] A. Gholampour, T. Ozbakkaloglu, *J. Mater. Sci.* **2020**, *55*, 829.
[47] S. Mortazavian, A. Fatemi, *Composites, Part B* **2015**, *72*, 116.
[48] N. C. Judd, *SAMPE J.* **1978**, *14*,1014.
[49] S. Panthapulakkal, M. Sain, *J. Polym. Environ.* **2006**, *14*, 265.
[50] Z. Ma, T. Yin, Z. Jiang, Y. Weng, C. Zhang, *Int. J. Biol. Macromol.* **2024**, *259*, 129319.
[51] N. Sato, T. Kurauchi, S. Sato, O. Kamigaito, *J. Mater. Sci.* **1991**, *26*, 3891.
[52] A. Fendler, M. Villanueva, E. Gimenez, J. Lagarón, *Cellulose* **2007**, *14*, 427.
[53] M. Mariano, N. El Kissi, A. Dufresne, *J. Polym. Sci., Part B: Polym. Phys.* **2014**, *52*, 791.
[54] S. Mooninta, S. Poompradub, P. Prasassarakich, *J. Polm. Environ.* **2020**, *28*, 3116.
[55] C. Maraveas, *Sustainability* **2019**, *11*, 6129.
[56] M.-A. Berthet, H. Angellier-Coussy, V. Chea, V. Guillard, E. Gastaldi, N. Gontard, *Composites, Part A* **2015**, *72*, 139.

